Witnessing entanglement in an undergraduate laboratory

Marisol N. Beck
Department of Physics, Harvey Mudd College, Claremont, California 91711

M. Beck[a)]
Department of Physics, Whitman College, Walla Walla, Washington 99362

(Received 3 August 2015; accepted 13 November 2015)

An entangled state of a two-particle system is a quantum state that cannot be separated, meaning it cannot be written as the product of states of the individual particles. One way to tell if a system is entangled is to use it to violate a Bell inequality (such as the Clauser-Horne-Shimony-Holt, CHSH, inequality), because entanglement is necessary for such a violation. However, there are other, easier-to-perform measurements that determine whether or not a system is entangled. An operator that corresponds to such a measurement is referred to as an entanglement witness. Here, we present the theory of witness operators and an undergraduate experiment that measures entanglement witnesses for the joint polarization state of two photons. We are able to produce states for which the expectation value of a witness operator is entangled by more than 300 standard deviations. In order to further examine the performance of these witness operators, we present a simple way to generate states that closely approximate Werner states, which have a controllable degree of entanglement.
[http://dx.doi.org/10.1119/1.4936623]

I. INTRODUCTION

Entanglement is one of the most important features that distinguishes quantum mechanics from classical mechanics. Entangled particles have correlations that are stronger than those allowed by classical physics. Entanglement is necessary for a diverse range of uniquely quantum mechanical effects such as quantum teleportation and quantum computing.[1,2]

Conceptually, to fully characterize an entangled state of a multi-particle system, including all of its correlations, one must describe the state of the entire system, not just the states of the individual particles. Mathematically, entangled states are those quantum states that cannot be written as the product of the states of the individual particles. Thus, if $|\psi_{\text{ent}}\rangle$ represents an entangled state of a bipartite system, then there do not exist any state vectors $|\psi_i\rangle_A$ (belonging to the Hilbert space H_A of A) and $|\psi_j\rangle_B$ (belonging to H_B) such that $|\psi_{\text{ent}}\rangle$ can be written as a direct product of $|\psi_i\rangle_A$ and $|\psi_j\rangle_B$. This means that

$$|\psi_{\text{ent}}\rangle \neq |\psi_i\rangle_A \otimes |\psi_j\rangle_B, \tag{1}$$

where $\otimes$ represents the direct product.

In Eq. (1), $|\psi_{\text{ent}}\rangle$ is an entangled pure state. It has been shown that for every bipartite, entangled pure state, there exists a Bell inequality that is violated.[3,4] Thus, there exists, at least in principle, a method to experimentally detect the entanglement. However, real experimental systems never exist in pure states. One must assume that the state of an experiment will yield a mixed state that must be described by density operator $\hat{\rho}$.[5,6] A mixed state is separable, and hence not entangled, if it can be written as a weighted sum of product states as in

$$\hat{\rho}_{\text{sep}} = \sum_k p_k \hat{\rho}_{Ak} \otimes \hat{\rho}_{Bk}, \tag{2}$$

where the p_k's are nonnegative real numbers, and the normalization condition is that $\Sigma_k\, p_k = 1$.

An observable that is able to detect entanglement is referred to as an entanglement witness.[7,8] Bell inequalities were (effectively) the first entanglement witnesses, but there are other, more efficient observables that are capable of revealing entanglement. For example, the minimum number of measurements needed to measure a Bell inequality for bipartite qubits (two 2-state particles) is four, whereas it is possible to construct an entanglement witness for these same qubits that requires only three measurements.[9] A violation of a Bell inequality rules out any local-realistic model. It is a very general result predicated on a minimum of assumptions about the underlying system being measured. Entanglement witnesses assume the validity of quantum mechanics (a much more restrictive set of assumptions) and merely seek to determine whether or not a particular system is entangled. Thus, it is not surprising that measuring entanglement witnesses would involve fewer measurements than a Bell inequality requires.

Experiments with entangled photons have been previously performed in undergraduate laboratories.[6,10–15] These experiments include tests of Bell inequalities, which prove that the states used in those experiments are entangled. However, we are unaware of any previous undergraduate experiments that measure the types of entanglement witnesses that we describe here. Furthermore, these witnesses require only three measurements (instead of four). In order to characterize the performance of our witness operators, we have developed a straightforward technique that generates states with a controllable degree of entanglement. These states closely approximate the class of states commonly known as Werner states.[16,17] Using these states, we demonstrate that our witness operators are able to detect entanglement in situations where the Clauser-Horne-Shimony-Holt (CHSH) inequality, the most commonly used Bell inequality, does not.[10,11,18]

We begin with a discussion of the theory of entanglement witnesses. We then present two witness operators that are capable of detecting entanglement in the joint polarization state of two photons. Finally, we describe undergraduate experiments that implement measurements of these operators and explore their performance.

II. THEORY

Here, we assume a familiarity with density operators, and note the reader will find a description of density operators in Refs. 5, 6, and 15.

A. Schmidt decomposition

Before discussing the general problem of identifying entanglement in arbitrary mixed state systems, let's first consider entanglement of pure states. Suppose that system A has dimension M and its Hilbert space H_A has basis vectors $|\alpha_i\rangle_A$. Similarly, system B has dimension N and H_B has basis vectors $|\beta_j\rangle_B$. An arbitrary pure state of the joint system can be written as

$$
\begin{aligned}
|\psi\rangle &= \sum_i^M \sum_j^N c_{ij} |\alpha_i\rangle_A \otimes |\beta_j\rangle_B \\
&= \sum_i^M \sum_j^N c_{ij} |\alpha_i \beta_j\rangle \,.
\end{aligned} \tag{3}
$$

The Schmidt decomposition (essentially the singular value decomposition) of $|\psi\rangle$ determines two new sets of vectors $|a_i\rangle_A$ and $|b_i\rangle_B$, such that[1,8]

$$
|\psi\rangle = \sum_i^R \lambda_i |a_i b_i\rangle. \tag{4}
$$

The number R is called the Schmidt rank of the state, and it is equal to the number of nonzero Schmidt coefficients λ_i $[R \leq \min(M, N)]$.[8] Note that while the sum in Eq. (4) is only over R states with nonzero Schmidt coefficients, the Schmidt decomposition determines $|a_i\rangle_A$'s and $|b_i\rangle_B$'s that form orthonormal bases for H_A and H_B, respectively. Furthermore, the Schmidt coefficients are real and positive.[8]

Equation (4) is a simplification over Eq. (3) because we have gone from a double sum to a single sum. The fact that the Schmidt decomposition of $|\psi\rangle$ exists is proved in Ref. 1. Note that the Schmidt decomposition only applies to pure states. The Schmidt rank of any pure product state is 1, while any pure state with $R > 1$ is entangled.

B. Witness operators

Here, we provide a description of witness operators that is sufficient for an understanding of our experiments. For a more complete discussion, see Refs. 4 and 8.

An observable $\hat{W}$ is an entanglement witness if

$$
\langle \hat{W} \rangle = \mathrm{Tr}(\hat{W} \hat{\rho}_{\mathrm{sep}}) \geq 0 \tag{5}
$$

for all separable states $\hat{\rho}_{\mathrm{sep}}$, and

$$
\langle \hat{W} \rangle = \mathrm{Tr}(\hat{W} \hat{\rho}_{\mathrm{ent}}) < 0 \tag{6}
$$

for at least one entangled state $\hat{\rho}_{\mathrm{ent}}$.[4,7,8] This means that if one measures $\langle \hat{W} \rangle < 0$, one knows that the state $\hat{\rho}$ is entangled.

There are different ways to construct witness operators. The technique we use is to note that if our experimentally produced state is "close enough" (in Hilbert space) to a particular entangled pure state $|\psi_{\mathrm{ent}}\rangle$, it will be entangled as well. As such we construct the witness operator[8]

$$
\hat{W} = \alpha \hat{1} - \hat{\rho}_{\mathrm{ent}} = \alpha \hat{1} - |\psi_{\mathrm{ent}}\rangle\langle\psi_{\mathrm{ent}}|. \tag{7}
$$

To see that this operator functions as a witness, note that

$$
\begin{aligned}
\langle \hat{W} \rangle &= \mathrm{Tr}(\alpha \hat{\rho}) - \mathrm{Tr}[(|\psi_{\mathrm{ent}}\rangle\langle\psi_{\mathrm{ent}}|)\hat{\rho}] \\
&= \alpha \mathrm{Tr}(\hat{\rho}) - \langle\psi_{\mathrm{ent}}|\hat{\rho}|\psi_{\mathrm{ent}}\rangle \\
&= \alpha - F,
\end{aligned} \tag{8}
$$

where we have used the normalization of the density operator and we have defined the fidelity F as $F = \langle\psi_{\mathrm{ent}}|\hat{\rho}|\psi_{\mathrm{ent}}\rangle$. The fidelity is a measure of the overlap of $|\psi_{\mathrm{ent}}\rangle$ and $\hat{\rho}$ in Hilbert space. We have $F = 1$ if $\hat{\rho} = |\psi_{\mathrm{ent}}\rangle\langle\psi_{\mathrm{ent}}|$ and $F = 0$ if $\hat{\rho}$ is orthogonal to $|\psi_{\mathrm{ent}}\rangle$. Assuming that the witness satisfies Eq. (5), if F exceeds the critical value α in Eq. (8), then $\langle \hat{W} \rangle$ is negative and we have identified $\hat{\rho}$ as being an entangled state.

In order to ensure that $\hat{W}$ defined in Eq. (7) meets the definition of an entanglement witness, the constant α is chosen to have the minimum value possible, constrained by the fact that $\hat{W}$ must satisfy Eq. (5) for all separable states, or

$$
\langle \hat{W} \rangle = \alpha\langle \hat{1} \rangle - \mathrm{Tr}(|\psi_{\mathrm{ent}}\rangle\langle\psi_{\mathrm{ent}}|\hat{\rho}_{\mathrm{sep}}) \geq 0. \tag{9}
$$

We thus require α to be given by

$$
\begin{aligned}
\alpha &= \max_{\hat{\rho}_{\mathrm{sep}}} \mathrm{Tr}(|\psi_{\mathrm{ent}}\rangle\langle\psi_{\mathrm{ent}}|\hat{\rho}_{\mathrm{sep}}) \\
&= \max_{\hat{\rho}_{\mathrm{sep}}} \langle\psi_{\mathrm{ent}}|\hat{\rho}_{\mathrm{sep}}|\psi_{\mathrm{ent}}\rangle \,,
\end{aligned} \tag{10}
$$

where the maximization is performed over the space of all separable states. The calculation of the maximum in Eq. (10) is performed in Appendix A, where it is shown that α is given by the square of the maximum Schmidt coefficient of $|\psi_{\mathrm{ent}}\rangle$, $\lambda_{\max}^2$.[8,19]

The two states we are interested in detecting are the Bell states

$$
|\Phi^\pm\rangle = \frac{1}{\sqrt{2}}(|HH\rangle \pm |VV\rangle). \tag{11}
$$

These are states of two photons in which $|HH\rangle$ is the state corresponding to both photons being horizontally polarized and $|VV\rangle$ corresponds to both photons being vertically polarized. The maximum Schmidt coefficient for either of these states is $1/\sqrt{2}$, and the witness operators that will detect them are

$$
\begin{aligned}
\hat{W}^\pm &= \frac{1}{2}\hat{1} - |\Phi^\pm\rangle\langle\Phi^\pm| \\
&= \frac{1}{2}\big[\hat{1} - |HH\rangle\langle HH| - |VV\rangle\langle VV| \\
&\quad \mp (|HH\rangle\langle VV| + |VV\rangle\langle HH|)\big].
\end{aligned} \tag{12}
$$

In the laboratory, we are able to perform local, projective measurements. The probability of obtaining a particular measurement outcome from such a measurement is given by the expectation value of the projector onto the state corresponding to the measurement. This is calculated using the density operator as

$$P(\psi) = \mathrm{Tr}(|\psi\rangle\langle\psi|\hat{\rho}). \quad (13)$$

If both Alice and Bob perform projective measurements on their respective particles, projection operators that correspond to these measurements take the form

$$|a\rangle_{AA}\langle a| \otimes |b\rangle_{BB}\langle b| = |ab\rangle\langle ab|. \quad (14)$$

The first two terms after the $\hat{1}$ in Eq. (12) take this form, but the two terms in parentheses don't, as they don't correspond to local, projective measurements. Thus, we must rewrite Eq. (12) in a form that shows us how to measure $\hat{W}^{\pm}$ by using such measurements. We accomplish this by recognizing that Alice and Bob are not limited to performing measurements in the horizontal-vertical basis.

We define the diagonal (D) and antidiagonal (A) (i.e., $\pm 45°$ linear), and the left-circular (L) and right-circular (R) polarization states as

$$|D\rangle = \frac{1}{\sqrt{2}}(|H\rangle + |V\rangle), \quad |A\rangle = \frac{1}{\sqrt{2}}(|H\rangle - |V\rangle) \quad (15)$$

and

$$|L\rangle = \frac{1}{\sqrt{2}}(|H\rangle + i|V\rangle), \quad |R\rangle = \frac{1}{\sqrt{2}}(|H\rangle - i|V\rangle). \quad (16)$$

Given these, it can be shown that it is possible to rewrite our witness operator in terms of local projection operators as

$$\hat{W}^{\pm} = \frac{1}{2}[\hat{1} - |HH\rangle\langle HH| - |VV\rangle\langle VV| \mp (|DD\rangle\langle DD| + |AA\rangle\langle AA| - |LL\rangle\langle LL| - |RR\rangle\langle RR|)]. \quad (17)$$

Finally, if we define $P(a,b)$ to be the joint probability that Alice measures her photon to have polarization a and Bob measures his photon to have polarization b, we find that the expectation values of the witness operators are

$$\langle\hat{W}^{\pm}\rangle = \frac{1}{2}\{1 - P(H,H) - P(V,V) \mp [P(D,D) + P(A,A) - P(L,L) - P(R,R)]\}. \quad (18)$$

III. EXPERIMENTS

Our experiments are similar to those performed in Ref. 9, but we use equipment that is currently found in many undergraduate laboratories.[6,10,13,20] The experimental apparatus is shown in Fig. 1. A 100-mW, 405-nm laser diode pumps a pair of type-I beta-barium borate crystals, whose axes are oriented at right angles with respect to each other. Down-converted photons pass through a series of wave plates and polarizing beam splitters before being focused onto multimode optical fibers and detected with single-photon counting modules. The half-wave plates in the down-converted beams in Fig. 1 are used for the measurements of the CHSH parameter S and are not needed for the measurement of the witnesses. During the witness measurement, we set their fast axes to 0° with respect to the horizontal, which has no effect on the witness measurements, and is simpler than removing them.

The polarization states of the down converted photon pairs are adjusted using techniques described in previous experiments.[6,10]

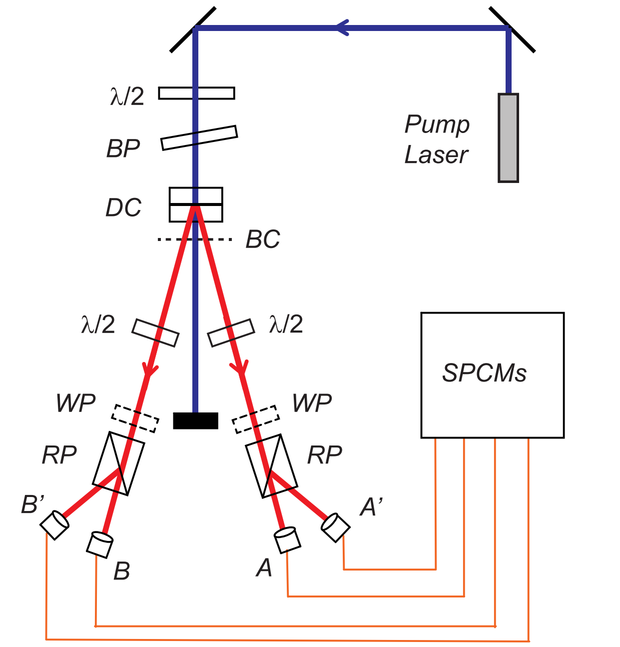

Fig. 1. (Color online) Schematic diagram of the experimental apparatus. Here, $\lambda/2$ denotes a half-wave plate, *BP* denotes a birefringent plate, *DC* denotes down conversion crystals, *BC* indicates a removable business card, *WP* denotes a removable wave plate, *RP* denotes a Rochon polarizer, and *SPCMs* are single-photon counting modules.

More details about the experimental apparatus can be found in Ref. 20. The states that we are trying to produce take the form

$$|\Phi(\phi)\rangle = \frac{1}{\sqrt{2}}\left(|HH\rangle + e^{i\phi}|VV\rangle\right). \quad (19)$$

However, our experimentally produced states are not pure. For the first set of experiments, we model our states as

$$\hat{\rho}_1 = p|\Phi(\phi)\rangle\langle\Phi(\phi)| + \frac{1-p}{2}(|HH\rangle\langle HH| + |VV\rangle\langle VV|). \quad (20)$$

This density operator represents our photons as being in the entangled state $|\Phi(\phi)\rangle$ with probability p, and in an equal mixture of the states $|HH\rangle$ and $|VV\rangle$ with probability $1-p$. A state of this type is produced, for example, if there is some temporal walk-off between the horizontal and vertical polarizations, which introduces a degree of distinguishability between them.

With the removable wave plates removed (see Fig. 1) horizontally polarized photon pairs are directed to detectors A and B, and vertically polarized photons are directed to detectors A' and B'. We can thus measure the probability of detecting horizontally polarized photon pairs as

$$P(H,H) = \frac{N_{AB}}{N_{AB} + N_{A'B} + N_{AB'} + N_{A'B'}}, \quad (21)$$

where N_{XY} is the number of coincidence photons detected at X and Y in a given time window. We can similarly determine $P(V,V)$ by replacing the numerator in this equation with $N_{A'B'}$. The probabilities of detecting diagonal and antidiagonal photon pairs are obtained by inserting half-wave plates oriented with their fast axes at 22.5° before the Rochon polarizers. To measure the circular polarization probabilities, we insert quarter-wave plates with their fast axes oriented at 45°. In our first set of experiments, we subtract the expected number of accidental coincidences from our data when using Eq. (21). These accidentals are due to the fact that for two independent detectors, there is some probability that both of them will register photons within a coincidence time window Δt just by pure random chance, even if they are illuminated with uncorrelated fields. It is not necessary to subtract accidental coincidences to observe entanglement, but the agreement between theory and experiment is improved if they are subtracted. A calculation of the expected number of accidental coincidences is given in Appendix B.

A. Varying the phase of the state

The birefringent plate in the pump beam is mounted on a tilt stage with a micrometer and used to adjust the relative phase ϕ of the pure-state component in our experimentally produced states of Eqs. (19) and (20). Note that $\phi = 0$ yields $|\Phi^+\rangle$ and $\phi = \pi$ yields $|\Phi^-\rangle$. The techniques described in Refs. 6 and 10 allow us to determine the tilt angles corresponding to $\phi = 0$ and $\phi = \pi$. We linearly extrapolate between these two tilt angles to set the phase angle of the state.

Figure 2 shows the experimental data for $\langle\hat{W}^\pm\rangle$ and S as we vary ϕ. The expectation values $\langle\hat{W}^\pm\rangle$ are obtained from the same data. The data for S are obtained separately, because it requires different measurement settings. Our technique for obtaining the measurements in Fig. 2 is to set the value of ϕ, measure $\langle\hat{W}^\pm\rangle$ and S one after the other, then change ϕ and repeat. In Fig. 2(a), we see that when we are creating states that are near $|\Phi^+\rangle$ (ϕ near 0), the

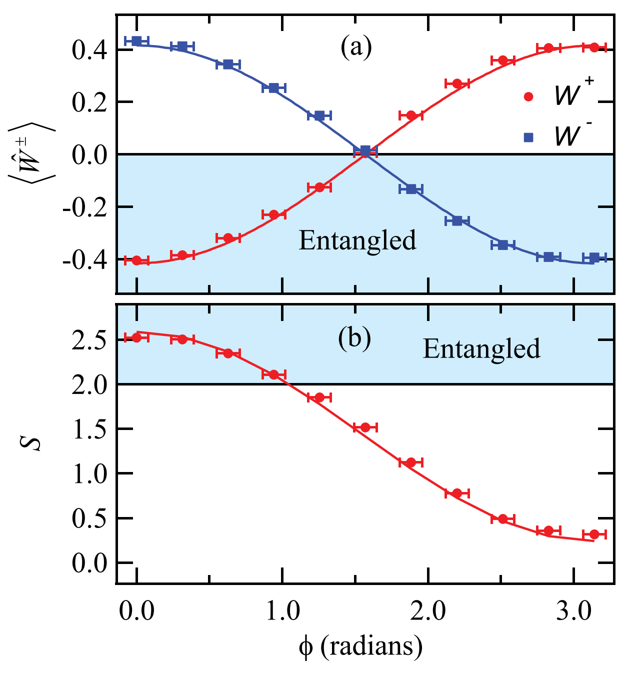

Fig. 2. (Color online) (a) $\langle\hat{W}^+\rangle$ (circles) and $\langle\hat{W}^-\rangle$ (squares) are plotted as a function of the entangled state phase ϕ. (b) The CHSH parameter S is plotted as a function of this same parameter. The points are experimental data while the solid lines are theoretical predictions. Statistical (vertical) error bars would be smaller than the markers and are not shown. Horizontal error bars are $\pm\pi/40$, which is our best estimate of how accurately we can set $\phi = 0$. All other phases are assumed to have the same error bars.

measurements of $\langle\hat{W}^+\rangle$ indicate that the state is entangled, while the measurements of $\langle\hat{W}^-\rangle$ do not. This is as we would expect, because $\hat{W}^+$ is constructed to witness this entangled state, while $\hat{W}^-$ is not. Their behavior switches as ϕ approaches π, and we are creating states near $|\Phi^-\rangle$. This demonstrates that the entanglement witness must be properly chosen to detect the state that is being produced in a particular experiment.

The version of the CHSH inequality that we use reveals entanglement in $|\Phi^+\rangle$ when $S > 2$. However, $\hat{W}^+$ does a "better" job of detecting this entanglement as $\langle\hat{W}^+\rangle$ indicates that the point at $\phi \cong 1.25$ rad is entangled, while S does not. We note that at $\phi = 0$ in Fig. 2 we have $\langle\hat{W}^+\rangle = -0.4042 \pm 0.0025$, which indicates that the state is entangled by over 160 standard deviations. For the same state, we have $S = 2.521 \pm 0.012$, which violates the CHSH inequality by 43 standard deviations. Note that the degree to which the measurements violate the classical inequalities are independent of experimental errors involved in creating particular states, because these inequalities are independent of the underlying state of the system.

In Appendix C, we calculate the theoretical predictions for $\langle\hat{W}^\pm\rangle$ and S, assuming the system is in state $\hat{\rho}_1$ of Eq. (20). This state contains the parameter p, which is the pure-state fraction contained in the experimentally measured states. We treat p as a free parameter, and use it to fit our data for $\langle\hat{W}^+\rangle$, and we find that $p = 0.83 \pm 0.01$. Once this value has been determined for $\langle\hat{W}^+\rangle$, we use it to determine the theoretical predictions for $\langle\hat{W}^-\rangle$ and S. Thus, a single parameter, obtained by fitting one set of data, allows us to fit all three sets of data in Fig. 2. This gives us confidence that the states we are producing in this experiment are reasonably well described by Eq. (20).

B. Varying the amount of entanglement

In order to test how our witness operators perform, it is useful to have a way of varying the degree of entanglement in our experimentally produced states. One class of states that have variable entanglement are Werner states, which take the form[16,17]

$$\hat{\rho}_W = p_W |\psi_{\text{ent}}\rangle\langle\psi_{\text{ent}}| + \frac{1 - p_W}{4}\hat{1}\,. \tag{22}$$

Werner states are in the pure entangled state $|\psi_{\text{ent}}\rangle$ with probability p_W, and in states of purely random polarization with probability $1 - p_W$.

Our technique for creating Werner states was inspired by Ref. 21, but is distinct. We set $\phi = 0$ so if our beams are unblocked we are producing states that approximate $|\psi_{\text{ent}}\rangle = |\Phi(\phi = 0)\rangle = |\Phi^+\rangle$. If we insert something to cause photons from our source to scatter multiple times, we produce randomly polarized photons. In our experiments, we use a standard, cardboard business card to produce scattered photons. It is inserted into the beam after the down-conversion crystal, as shown in Fig. 1. The photons we detect with the business card in place are not primarily down-converted photons, but are now due to the pump beam's interaction with the card. They are either scattered pump photons that make it through the colored glass filters intended to filter them out or near infra-red fluorescence from the card. In either case, they have random polarization and statistics.

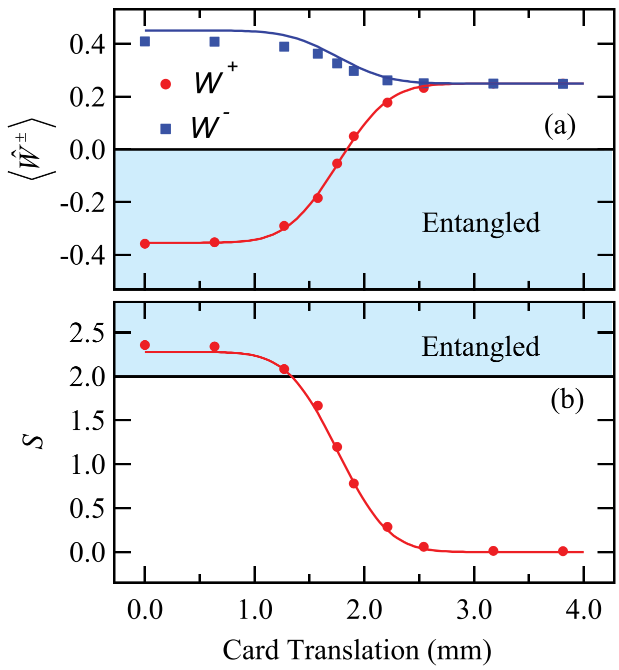

Fig. 3. (Color online) (a) $\langle \hat{W}^+ \rangle$ (circles) and $\langle \hat{W}^- \rangle$ (squares) are plotted as a function of the translation of the business card. (b) The CHSH parameter S is plotted as a function of this same parameter. The points are experimental data while the solid lines are theoretical predictions. Statistical (vertical) error bars would be smaller than the markers and are not shown.

We place the card at the proper distance from the crystal to ensure that the average coincidence count rates on our detectors are approximately the same as with the card removed. However, with the card fully inserted, all of the measured coincidences are accidental. Thus, we cannot subtract accidental coincidences for this experiment or we would have an average of 0 coincidences with the card fully inserted. To adjust the degree of entanglement, or the parameter p_W in Eq. (22), we put our business card on a translation stage that moves the card in a controllable manner in the vertical direction; the larger the fraction of the beam that is blocked by the card, the less entanglement in our states.

In Fig. 3, we show our experimental measurements of $\langle \hat{W}^{\pm} \rangle$ and S as we vary the translation of the business card, and hence the degree of entanglement. We see that when the card is removed both $\langle \hat{W}^+ \rangle$ and S indicate entanglement, while $\langle \hat{W}^- \rangle$ does not. Since the pure state contribution in $\hat{\rho}_W$ is $|\Phi^+\rangle$, the results shown in Fig. 3 are what we would expect. With the card completely out of the beam, we find $\langle \hat{W}^+ \rangle = -0.3577 \pm 0.0009$, which indicates that the state is entangled by over 300 standard deviations, and S=2.358 $\pm$0.008, which violates the CHSH inequality by 44 standard deviations. The mean values of these parameters indicate that the purity of the pure-state component of our states in this experiment is not as large as it was in the experiment described in Fig. 2. We attribute this, at least in part, to the fact that we are not subtracting accidental coincidences in this experiment. This absence of subtraction is necessary to ensure that we properly characterize the behavior of the state with the card fully inserted (the measured photons come from the scattering source and have random polarization). However, not subtracting the accidentals decreases the agreement between theory and experiment when the card is removed (the measured photons come from the down conversion source and are polarization entangled).

As is seen in Fig. 3, the further the card is inserted into the beam, the less entanglement we measure. Once the beam is completely blocked we find $\langle \hat{W}^{\pm} \rangle \cong 1/4$ and $S \cong 0$, which is what we would expect for randomly polarized photons.

In Fig. 3, $\langle \hat{W}^+ \rangle$ indicates that five of the measured states are entangled, while S indicates that only three of them are entangled. Thus, in this case $\hat{W}^+$ is better at detecting weak entanglement than S. This is probably not surprising, as $\hat{W}^+$ was specifically designed for this task, while S was designed to solve the more general problem of ruling out local hidden-variable theories. In some sense, entanglement witnesses are the "right tool for the job" of detecting entanglement, at least when compared to Bell inequalities.

The theoretical predictions for our measured quantities are presented in Appendix C and are plotted in Fig. 3. Once again we fit the theory to the data for $\langle \hat{W}^+ \rangle$ and use the same fit parameters to present the theoretical predictions for all of the other measured quantities. We see that the theory works well for $\langle \hat{W}^+ \rangle$, and reasonably well for S, but not as well for $\langle \hat{W}^- \rangle$. We attribute this disagreement to two factors. One is that we are not subtracting accidental coincidences. The other is that the theoretical prediction for a Werner state $\hat{\rho}_W$ has the state approaching a pure state as $p_W \rightarrow 1$, but in our experiments this state is actually converging to a state of the form in Eq. (20). Thus, while we have implemented a method for creating states having an adjustable degree of entanglement, these states are only approximately Werner states.

IV. CONCLUSIONS

We have experimentally measured the expectation values of two different entanglement witness operators $\langle \hat{W}^{\pm} \rangle$ in an experiment that is suitable for an undergraduate laboratory. We have also compared these measurements to measurements of the CHSH parameter S. Determining $\langle \hat{W}^{\pm} \rangle$ is "easier" in that they require only three measurements, as compared to four measurements for S. The witness operators also indicate entanglement for weakly entangled states that S does not, and they yield a larger violation of classical physics (in terms of the number of standard deviations a classical inequality is violated). As such, we conclude that if one is interested only in whether or not a state is entangled, and not in violations of local realism, entanglement witnesses are a better tool than Bell inequalities.

In order to perform our experiments, we have developed a very simple technique for creating states having an adjustable amount of entanglement, which involves translating a business card into the detected beams. The states produced in this manner approximate Werner states.

ACKNOWLEDGMENTS

The authors thank M. Gresham and M. Schlosshauer for careful readings of our manuscript. This work was supported by Whitman College.

APPENDIX A: CALCULATING THE WITNESS OPERATORS

Here, we derive the expression for the witness operators given in Eq. (17). This derivation is based primarily on information in Refs. 8 and 19.

Begin by writing the density operator $\hat{\rho}_{Ak}$ in Eq. (2) as a weighted sum of pure-state density operators

$$\hat{\rho}_{Ak} = \sum_i a_{ki} |i\rangle_{AA}\langle i|. \tag{A1}$$

The sum is over states in which the system may be prepared. The $|i\rangle_A$'s need not form a basis, nor do they need to be orthogonal. We also write a similar expression for $\hat{\rho}_{Bk}$. The density operator $\hat{\rho}_{\text{sep}}$ in Eq. (2) can then be rewritten as

$$\begin{aligned}\hat{\rho}_{\text{sep}} &= \sum_k p_k \sum_i \sum_j a_{ki} b_{kj} (|i\rangle_{AA}\langle i|) \otimes (|j\rangle_{BB}\langle j|) \\ &= \sum_i \sum_j \left(\sum_k p_k a_{ki} b_{kj} \right) |ij\rangle\langle ij| \,.\end{aligned} \tag{A2}$$

Defining p_{ij} to be equal to the sum in parentheses, we find

$$\hat{\rho}_{\text{sep}} = \sum_i \sum_j p_{ij} |ij\rangle\langle ij| \,. \tag{A3}$$

Using Eq. (A3), Eq. (10) becomes

$$\alpha = \max_{p_{ij},|ij\rangle} \sum_i \sum_j p_{ij} |\langle \psi_{\text{ent}} | ij\rangle|^2, \tag{A4}$$

where we are maximizing over separable states (expressed as combinations of p_{ij} and $|ij\rangle$). Let $|\langle \psi_{\text{ent}}|ij\rangle|^2_{\max}$ be the maximum value of $|\langle \psi_{\text{ent}}|ij\rangle|^2$, for all values of i and j. It must then be the case that

$$\alpha \le \max_{p_{ij},|ij\rangle} \sum_i \sum_j p_{ij} |\langle \psi_{\text{ent}} | ij\rangle|^2_{\max}. \tag{A5}$$

Since $|\langle \psi_{\text{ent}}|ij\rangle|^2_{\max}$ is constant it can be pulled out of the sum, yielding

$$\begin{aligned}\alpha &\le \max_{p_{ij},|ij\rangle} |\langle \psi_{\text{ent}} | ij\rangle|^2_{\max} \sum_i \sum_j p_{ij} \\ &= \max_{|ij\rangle} |\langle \psi_{\text{ent}} | ij\rangle|^2 \,,\end{aligned} \tag{A6}$$

where we have used the normalization of the p_{ij}'s.

Note that we haven't specified the states $|ij\rangle$ that we are maximizing $|\langle \psi_{\text{ent}}|ij\rangle|^2$ over. Thus, we have gone from maximizing $\langle \psi_{\text{ent}}|\hat{\rho}_{\text{sep}}|\psi_{\text{ent}}\rangle$ over all separable states $\hat{\rho}_{\text{sep}}$ to maximizing $|\langle \psi_{\text{ent}}|ij\rangle|^2$ over all possible states $|ij\rangle$. This has helped because the states $|ij\rangle = |i\rangle_A \otimes |j\rangle_B$ are pure product states. Thus, we've reduced our problem from maximizing over all separable states (including separable mixed states) to maximizing over all pure product states.

To perform the maximization in Eq. (A6), we start by noting that we can write the entangled state in its Schmidt decomposition of Eq. (4). We can also write the pure product state $|ij\rangle$ in the basis that is determined by the Schmidt decomposition of $|\psi_{\text{ent}}\rangle$ (although it is not necessarily diagonal in this basis) as

$$\begin{aligned}|ij\rangle &= \left(\sum_m^M c_m^a |a_m\rangle_A \right) \otimes \left(\sum_n^N c_n^b |b_n\rangle_B \right) \\ &= \sum_m^M \sum_n^N c_m^a c_n^b |a_m b_n\rangle \,.\end{aligned} \tag{A7}$$

Because the states are normalized, we have

$$\sum_m^M |c_m^a|^2 = \sum_n^N |c_n^b|^2 = 1. \tag{A8}$$

Using the fact that the Schmidt coefficients are real and positive, Eq. (A6) becomes

$$\begin{aligned}\alpha &\le \max_{c_m^a, c_n^b} \left| \left(\sum_k^R \lambda_k \langle a_k b_k| \right) \left(\sum_m^M \sum_n^N c_m^a c_n^b |a_m b_n\rangle \right) \right|^2 \\ &= \max_{c_k^a, c_k^b} \left| \sum_k^R \lambda_k c_k^a c_k^b \right|^2 \\ &\le \max_{c_k^a, c_k^b} \lambda_{\max}^2 \left| \sum_k^R c_k^a c_k^b \right|^2,\end{aligned} \tag{A9}$$

where, again, $\lambda_{\max}^2$ is the square of the maximum Schmidt coefficient of $|\psi_{\text{ent}}\rangle$. We now use the Cauchy-Schwarz inequality and obtain

$$\begin{aligned}\alpha &\le \max_{c_k^a, c_k^b} \lambda_{\max}^2 \sum_k^R |c_k^a|^2 \sum_k^R |c_k^b|^2 \\ &\le \lambda_{\max}^2,\end{aligned} \tag{A10}$$

where we have used Eq. (A8), and the fact that $R \le \min(M,N)$. Choosing equality on this condition guarantees that Eq. (5) is satisfied. While the proof presented here shows that $\alpha \le \lambda_{\max}^2$, and equality is chosen to safely guarantee that our witness operator is positive for separable states, a more general proof shows that indeed $\alpha = \lambda_{\max}^2$.[19]

APPENDIX B: ACCIDENTAL COINCIDENCES

Here, we calculate the expected number of accidental coincidences due to the finite time window used for coincidence detection.

If the detection probability is small, we can write the probability of the detection of a photon in time window Δt as the average rate of detections R_A multiplied by Δt, as $P_A = R_A \Delta t$. The rate of detections is the total number of detections N_A divided by the total counting time T, or $R_A = N_A/T$. The same mathematics applies to detections at B, and coincidence detections at A and B. If the detections at A and B are independent, the probability of coincidence detections is simply that due to random accidentals, and it factorizes as

$$\begin{aligned}P_{AB} &= P_A P_B \\ R_{AB}\Delta t &= (R_A \Delta t)(R_B \Delta t) \\ \frac{N_{AB}\Delta t}{T} &= \frac{(N_A \Delta t)(N_B \Delta t)}{T^2} \,.\end{aligned} \tag{B1}$$

Solving for the expected number of accidental coincidences yields

$$N_{AB} = \frac{N_A N_B \Delta t}{T}. \tag{B2}$$

Thus, from the measured coincidence window, the counting time, and the counts on two detectors, we can estimate the expected number of accidental coincidences and subtract it from our measured value. We do this for all four sets of measured coincidences in Eq. (21) when determining the probabilities in our first experiment.

The coincidence window is measured by illuminating the detectors with light that is known to be random and uncorrelated. In our case, this is scattered light from a business card inserted into the pump beam. Each coincidence window is measured separately, and all are approximately 8 ns.

APPENDIX C: THEORETICAL PREDICTIONS

Here, we derive the theoretical predictions that are presented in Figs. 2 and 3.

Start with witness operators in the form of Eq. (12), and assume we are in the state $\hat{\rho}_{\rm pure} = |\Phi(\phi)\rangle\langle\Phi(\phi)|$, where $|\Phi(\phi)\rangle$ is given by Eq. (19). The expectation values of the witness operators are then

$$\begin{aligned}\langle\hat{W}^{\pm}\rangle_{\rm pure} &= {\rm Tr}\left[\left(\frac{1}{2}\hat{1} - |\Phi^{\pm}\rangle\langle\Phi^{\pm}|\right)\hat{\rho}_{\rm pure}\right]\\ &= \frac{1}{2} - {\rm Tr}\left[\left(|\Phi^{\pm}\rangle\langle\Phi^{\pm}|\right)\hat{\rho}_{\rm pure}\right]\\ &= \frac{1}{2} - |\langle\Phi^{\pm}|\Phi(\phi)\rangle|^2 . \end{aligned}\tag{C1}$$

Expanding, this becomes

$$\begin{aligned}\langle\hat{W}^{\pm}\rangle_{\rm pure} &= \frac{1}{2} - \frac{1}{4}|(\langle HH|\pm\langle VV|)\left(|HH\rangle + e^{i\phi}|VV\rangle\right)|^2\\ &= \frac{1}{2} - \frac{1}{4}|1\pm e^{i\phi}|^2\\ &= \mp\frac{1}{2}\cos\phi . \end{aligned}\tag{C2}$$

Now assume we are in state $\hat{\rho}_1$ of Eq. (20). The expectation value for the witness operators is

$$\begin{aligned}\langle\hat{W}^{\pm}\rangle &= {\rm Tr}\left(\hat{W}^{\pm}\hat{\rho}_1\right)\\ &= p{\rm Tr}\left[\hat{W}^{\pm}\hat{\rho}_{\rm pure}\right] + \frac{1-p}{2}{\rm Tr}\\ &\quad\times\left[\hat{W}^{\pm}(|HH\rangle\langle HH| + |VV\rangle\langle VV|)\right]\\ &= p\langle\hat{W}^{\pm}\rangle_{\rm pure} + \frac{1-p}{2}{\rm Tr}\left[\left(\frac{1}{2}\hat{1} - |\Phi^{\pm}\rangle\langle\Phi^{\pm}|\right)\right.\\ &\quad\times(|HH\rangle\langle HH| + |VV\rangle\langle VV|)]. \end{aligned}\tag{C3}$$

Using Eq. (C2) and expanding, we find

$$\begin{aligned}\langle\hat{W}^{\pm}\rangle &= \mp\frac{p}{2}\cos\phi + \frac{1-p}{2}\\ &\quad\times\left\{\left[\left(\frac{1}{2}\right){\rm Tr}(|HH\rangle\langle HH| + |VV\rangle\langle VV|)\right]\right.\\ &\quad\left.-\left(|\langle HH|\Phi^{\pm}\rangle|^2 + |\langle VV|\Phi^{\pm}\rangle|^2\right)\right\}\\ &= \mp\frac{p}{2}\cos\phi + \frac{1-p}{2}\left\{\left(\frac{1}{2}+\frac{1}{2}\right) - \left(\frac{1}{2}+\frac{1}{2}\right)\right\}\\ &= \mp\frac{p}{2}\cos\phi. \end{aligned}\tag{C4}$$

This is the prediction for $\langle\hat{W}^{\pm}\rangle$ that is used in Fig. 2.

Next we find the prediction for the CHSH parameter S, assuming the system is in the state $\hat{\rho}_1$ of Eq. (20). First define the state $|\theta\rangle$, which is linearly polarized at an angle θ with respect to the horizontal as

$$|\theta\rangle = \cos\theta|H\rangle + \sin\theta|V\rangle. \tag{C5}$$

Next, we define the Hermitian polarization operator $\hat{\wp}_\theta$, which corresponds to a measurement of this polarization. States found to be polarized along θ have eigenvalue $+1$, while states polarized along $\theta^{\perp} = \theta + \pi/2$, which is perpendicular to θ, have eigenvalue -1. As such, we can write $\hat{\wp}_\theta$ as

$$\hat{\wp}_\theta = |\theta\rangle\langle\theta| - |\theta^{\perp}\rangle\langle\theta^{\perp}|. \tag{C6}$$

Using this and Eq. (C5), it is possible to show that the matrix elements of $\hat{\wp}_\theta$ in the horizontal-vertical basis are

$$\langle H|\hat{\wp}_\theta|H\rangle = \cos 2\theta, \tag{C7}$$

$$\langle V|\hat{\wp}_\theta|V\rangle = -\cos 2\theta, \tag{C8}$$

and

$$\langle H|\hat{\wp}_\theta|V\rangle = \langle V|\hat{\wp}_\theta|H\rangle = \sin 2\theta. \tag{C9}$$

The joint polarization operator corresponding to Alice measuring polarization θ_A and Bob measuring polarization θ_B is $\hat{\wp}^{AB}_{\theta_A\theta_B} = \hat{\wp}^{A}_{\theta_A}\hat{\wp}^{B}_{\theta_B}$, and the expectation value of a measurement corresponding to $\hat{\wp}^{AB}_{\theta_A\theta_B}$, assuming the system is in the pure state $|\Phi(\phi)\rangle$, is

$$\begin{aligned}E_{\rm pure}(\theta_A,\theta_B,\phi) &= \langle\Phi(\phi)|\hat{\wp}^{AB}_{\theta_A\theta_B}|\Phi(\phi)\rangle = \frac{1}{2}\left[\langle HH|\hat{\wp}^{A}_{\theta_A}\hat{\wp}^{B}_{\theta_B}|HH\rangle + \langle VV|\hat{\wp}^{A}_{\theta_A}\hat{\wp}^{B}_{\theta_B}|VV\rangle + e^{-i\phi}\langle VV|\hat{\wp}^{A}_{\theta_A}\hat{\wp}^{B}_{\theta_B}|HH\rangle\right.\\ &\quad\left. + e^{i\phi}\langle HH|\hat{\wp}^{A}_{\theta_A}\hat{\wp}^{B}_{\theta_B}|VV\rangle\right] = \cos 2\theta_A\cos 2\theta_B + \sin 2\theta_A\sin 2\theta_B\cos\phi . \end{aligned}\tag{C10}$$

We note that this expectation value explicitly depends on the phase angle ϕ in the state $|\Phi(\phi)\rangle$.

Now assume we are in state $\hat{\rho}_1$ of Eq. (20), yielding

$$\begin{aligned}E(\theta_A,\theta_B,\phi) &= {\rm Tr}\left[\hat{\wp}^{A}_{\theta_A}\hat{\wp}^{B}_{\theta_B}\hat{\rho}^{1}\right] = p{\rm Tr}\left[\hat{\wp}^{A}_{\theta_A}\hat{\wp}^{B}_{\theta_B}|\Phi(\phi)\rangle\langle\Phi(\phi)|\right] + \frac{1-p}{2}{\rm Tr}\left[\hat{\wp}^{A}_{\theta_A}\hat{\wp}^{B}_{\theta_B}(|HH\rangle\langle HH| + |VV\rangle\langle VV|)\right]\\ &= pE_{\rm pure}(\theta_A,\theta_B,\phi) + \frac{1-p}{2}\left(\langle HH|\hat{\wp}^{A}_{\theta_A}\hat{\wp}^{B}_{\theta_B}|HH\rangle + \langle VV|\hat{\wp}^{A}_{\theta_A}\hat{\wp}^{B}_{\theta_B}|VV\rangle\right). \end{aligned}\tag{C11}$$

Using the matrix elements of $\hat{\wp}_\theta$ and Eq. (C10), we find

$$\begin{aligned} E(\theta_A, \theta_B, \phi) &= p(\cos 2\theta_A \cos 2\theta_B + \sin 2\theta_A \sin 2\theta_B \cos\phi) \\ &\quad + (1-p)(\cos 2\theta_A \cos 2\theta_B) \\ &= \cos 2\theta_A \cos 2\theta_B + p \sin 2\theta_A \sin 2\theta_B \cos\phi\,. \end{aligned} \tag{C12}$$

The CHSH parameter, as a function of the phase ϕ, is then[11,18]

$$\begin{aligned} S(\phi) &= E\left(-\frac{\pi}{4}, -\frac{\pi}{8}, \phi\right) - E\left(-\frac{\pi}{4}, \frac{\pi}{8}, \phi\right) \\ &\quad + E\left(0, -\frac{\pi}{8}, \phi\right) + E\left(0, \frac{\pi}{8}, \phi\right). \end{aligned} \tag{C13}$$

This is the prediction for S that is used in Fig. 2.

The expectation values of our witnesses, for the Werner state in Eq. (22), are given by

$$\begin{aligned} \langle \hat{W}^{\pm} \rangle &= \mathrm{Tr}\left(\hat{W}^{\pm} \hat{\rho}_W\right) \\ &= p_W \mathrm{Tr}\left(\hat{W}^{\pm} \hat{\rho}_{\text{pure}}\right) + \frac{1-p_W}{4} \mathrm{Tr}\left(\hat{W}^{\pm}\right) \\ &= p_W \langle \hat{W}^{\pm} \rangle_{\text{pure}} + \frac{1-p_W}{4} \\ &\quad \times \left[\frac{1}{2}\mathrm{Tr}(\hat{1}) - \mathrm{Tr}\left[|\Phi^{\pm}\rangle\langle\Phi^{\pm}|\right]\right]. \end{aligned} \tag{C14}$$

Using Eq. (C2), $\mathrm{Tr}(\hat{1}) = 4$, and the fact that the trace of a normalized state is 1 yields

$$\langle \hat{W}^{\pm} \rangle = \mp \frac{p_W}{2} \cos\phi + \frac{1-p_W}{2} - \frac{1-p_W}{4}. \tag{C15}$$

Finally, we note that when we are performing the measurements for the Werner state, we set $\phi = 0$, so

$$\langle \hat{W}^{\pm} \rangle = \mp \frac{p_W}{2} + \frac{1-p_W}{4}. \tag{C16}$$

The expectation value of $\hat{\wp}^{AB}_{\theta_A\theta_B}$, assuming the system to be in a Werner state with $\phi = 0$, is

$$\begin{aligned} E(\theta_A, \theta_B) &= \mathrm{Tr}\left[\hat{\wp}^A_{\theta_A} \hat{\wp}^B_{\theta_B} \hat{\rho}_W\right] \\ &= p_W \mathrm{Tr}\left[\hat{\wp}^A_{\theta_A} \hat{\wp}^B_{\theta_B} |\Phi(0)\rangle\langle\Phi(0)|\right] \\ &\quad + \frac{1-p_W}{4} \mathrm{Tr}\left[\hat{\wp}^A_{\theta_A} \hat{\wp}^B_{\theta_B}\right] \\ &= p_W E_{\text{pure}}(\theta_A, \theta_B, 0) + \frac{1-p_W}{4} \mathrm{Tr}\left[\hat{\wp}^A_{\theta_A} \hat{\wp}^B_{\theta_B}\right]. \end{aligned} \tag{C17}$$

Computing the trace in the horizontal-vertical basis, and using the matrix elements of $\hat{\wp}_\theta$, we find

$$\begin{aligned} E(\theta_A, \theta_B) &= p_W E_{\text{pure}}(\theta_A, \theta_B, 0) + \frac{1-p_W}{4} \\ &\quad \times \left[\langle HH|\hat{\wp}^A_{\theta_A} \hat{\wp}^B_{\theta_B}|HH\rangle + \langle HV|\hat{\wp}^A_{\theta_A} \hat{\wp}^B_{\theta_B}|HV\rangle \right. \\ &\quad \left. + \langle VH|\hat{\wp}^A_{\theta_A} \hat{\wp}^B_{\theta_B}|VH\rangle + \langle VV|\hat{\wp}^A_{\theta_A} \hat{\wp}^B_{\theta_B}|VV\rangle\right] \\ &= p_W E_{\text{pure}}(\theta_A, \theta_B, 0)\,. \end{aligned} \tag{C18}$$

Since S is just a linear combination of expectation values, we find that for a Werner state

$$S_W = p_W S_{\text{pure}} = p_W 2\sqrt{2}, \tag{C19}$$

where we have used the value of S obtained when the system is prepared in state $|\Phi(0)\rangle = |\Phi^+\rangle$.

To obtain the fits to the data in Fig. 3, we first invert Eq. (C16) to find p_W in terms of $\langle \hat{W}^+ \rangle$, so that we can determine the value of p_W for each of the experimental measurements of $\langle \hat{W}^+ \rangle$ (i.e., as a function of the translation of the business card). The pure state fraction p_W should be proportional to the area of the unblocked portion of the beams, and for Gaussian beams this area should be an error function. We thus fit p_W to an error function, with the fit parameters being the width of the beam, the location of the center of the beam, and the maximum pure state fraction. This fit is then used to determine the theoretical predictions for $\langle \hat{W}^{\pm} \rangle$ and S of Eqs. (C16) and (C19) that are used in Fig. 3.

[a]Electronic mail: beckmk@whitman.edu

[1]M. A. Nielsen and I. L. Chuang, *Quantum Computation and Quantum Information* (Cambridge U.P., Cambridge, 2000).

[2]T. D. Ladd *et al.*, "Quantum computers," Nature **464**, 45–53 (2010).

[3]N. Gisin and A. Peres, "Maximal violation of Bell's inequality for arbitrarily large spin," Phys. Lett. A **162**, 15–17 (1992).

[4]B. M. Terhal, "Detecting quantum entanglement," Theor. Comput. Sci. **287**, 313–335 (2002).

[5]C. Cohen-Tannoudji, B. Diu, and F. Laloë, *Quantum Mechanics* (John Wiley and Sons, New York, 1977), pp. 295–307.

[6]M. Beck, *Quantum Mechanics: Theory and Experiment* (Oxford U.P., Oxford, 2012).

[7]M. Horodecki, P. Horodecki, and R. Horodecki, "Separability of mixed states: necessary and sufficient conditions," Phys. Lett. A **223**, 1–8 (1996).

[8]O. Gühne and G. Toth, "Entanglement detection," Phys. Rep. **474**, 1–75 (2009).

[9]M. Barbieri *et al.*, "Detection of entanglement with polarized photons: Experimental realization of an entanglement witness," Phys. Rev. Lett. **91**, 227901-1–4 (2003).

[10]D. Dehlinger and M. W. Mitchell, "Entangled photon apparatus for the undergraduate laboratory," Am. J. Phys. **70**, 898–902 (2002).

[11]D. Dehlinger and M. W. Mitchell, "Entangled photons, nonlocality, and Bell inequalities in the undergraduate laboratory," Am. J. Phys. **70**, 903–910 (2002).

[12]J. A. Carlson, M. D. Olmstead, and M. Beck, "Quantum mysteries tested: An experiment implementing Hardy's test of local realism," Am. J. Phys. **74**, 180–186 (2006).

[13]E. J. Galvez, "Qubit quantum mechanics with correlated-photon experiments," Am. J. Phys. **78**, 510–519 (2010).

[14]J. Carvioto-Lagos *et al.*, "The Hong-Ou-Mandel interferometer in the undergraduate laboratory," Eur. J. Phys. **33**, 1843–1850 (2012).

[15]E. Dederick and M. Beck, "Exploring entanglement with the help of quantum state measurement," Am. J. Phys. **82**, 962–971 (2014).

[16]R. F. Werner, "Quantum states with Einstein-Podolsky-Rosen correlations admitting a hidden-variable model," Phys. Rev. A **40**, 4277–4281 (1989).

[17]M. Barbieri, F. De Martini, G. Di Nepi, and P. Mataloni, "Generation and characterization of Werner states and maximally entangled mixed states by a universal source of entanglement," Phys. Rev. Lett. **92**, 177901-1–4 (2004).

[18]J. F. Clauser, M. A. Horne, A. Shimony, and R. A. Holt, "Proposed experiment to test local hidden-variable theories," Phys. Rev. Lett. **23**, 880–884 (1969).

[19]M. Bourennane *et al.*, "Experimental detection of multipartite entanglement using witness operators," Phys. Rev. Lett. **92**, 087902-1–4 (2004).

[20]Modern Quantum Mechanics Experiments for Undergraduates, <http://www.whitman.edu/∼beckmk/QM/>. This website details several experiments exploring quantum mechanics that have been developed for undergraduates.

[21]H. Kumano *et al.*, "Characterization of two-photon polarization mixed states generated from entangled-classical hybrid photon source," Opt. Express **19**, 14249–14259 (2011).